Mausam, (1990), **41**, 1, 11-20

551.461.22:551.553.21 (5)

On the intraseasonal variations of the Asiatic summer monsoon

CHANDRASEKHARA R. KONDRAGUNTA

University of Hawaii, Honolulu

(*Received 25 January 1989*)

सार — उत्तरी गोलार्ध की आठ ग्रीष्म ऋतुओं (1978 को छोड़कर 1975-83 की 1 मई से 30 सितम्बर तक) के अन्तर्गत बहिर्गामी दीर्घतरंग विकिरण (ब.दी.वि.) का प्रयोग करते हुए, एशियाई ग्रीष्म मानसून के अंत: मौसम उतार-चढ़ावों का पता लगाया गया। यह अंत: मौसमी विभिन्नता भूमध्य रेखीय हिन्द महासागर और उत्तर-पश्चिम प्रशांत में बहुत अधिक पाई जाती है। भारत में, भूमध्य रेखीय हिन्द महासागर और उत्तर-पश्चिम प्रशांत में ब. दी. वि. उतार-चढ़ाव 30–60 दिन, 10–20 दिन और 10 दिन से कम समय मानों पर अधिकतम स्पैक्ट्रम प्रदर्शित करते हैं। यह अध्ययन अन्तरवार्षिक विविधता के साथ सहयोजित अंत:मौसमी विभिन्नता को भी प्रकट करता है। भारत में सामान्यत: कम ग्रीष्म वर्षा के वर्ष 30–60 दोलन के साथ, सामान्य के निकट ग्रीष्म वर्षा के वर्ष 30–60 दिन और 10–20 दिन के दोलनों और सामान्य से अधिक वर्षा के, वर्ष 10 दिनों से कम के दोलनों के साथ सहसंबंधित होते हैं।

सम्पूर्ण एशियाई ग्रीष्म मानसून क्षेत्र के लिए आनुभविक लांबिक फलन (आ. लां. फ.) विश्लेषण किया गया। प्रथम चार आ. लां. फ. (इ. ओ. एफ.) गुणांक कुल विभिन्नता के 15 प्रतिशत को बताते हैं। आ. लां. फ. (इ. ओ. एफ.) विश्लेषण एशियाई ग्रीष्म मानसून क्षेत्र में कम से कम तीन समय मानों अर्थात् 30–60 दिन, 10–20 दिन और 10 दिन से कम के दोलनों की विद्यमानता की पुष्टि करता है।

ABSTRACT. Intraseasonal fluctuations of the Asiatic summer monsoon are investigated using Outgoing Longwave Radiation (OLR) covering eight northern hemisphere summers (1 May to 30 September 1975-83, except 1978). The intraseasonal variance is large in the equatorial Indian Ocean and the northwest Pacific. OLR fluctuations in the equatorial Indian Ocean, over India and the northwest Pacific show spectral peaks on time scales 30-60 day, 10-20 day and less than 10 days. This study also reveals intraseasonal variation associated with the interannual variation. Over India below normal summer rainfall years are associated with 30-60 oscillation, near normal summer rainfall years are associated with 30-60 day and 10-20 day oscillations and above normal rainfall years are associated with oscillations less than 10 days.

Empirical Orthogonal Function (EOF) analysis has been carried out for the whole Asiatic summer monsoon domain. The first four EOF coefficients explain 15% of the total variance. EOF analysis confirms existence of oscillations at least on three time scales, *viz.*, 30-60 day, 10-20 day and less than 10 days over the Asian summer monsoon region.

1. Introduction

Many studies on intraseasonal variation of the northern hemisphere summer revealed periodicities around 5-day, 15-day and 45 days. Murakami (1980) through empirical orthogonal function analysis of Outgoing Longwave Radiation (OLR) during northern hemisphere summers of 1974-77, showed a 20–30 day perturbation. Through spectrum analysis of a near normal monsoon system Krishnamurti and Bhalme (1976) noticed oscillations on the time scales of 15-day and 2-6 day. They attributed these oscillations to the active and break phases of the Indian summer monsoon.

Cadet (1983) analyzed the surface observations over the Indian Ocean on the intraseasonal time scale. His results show a westward propagating mode with 20–40 day periodicity over the tropical Indian Ocean along with the northward propagating one over the eastern Indian Ocean. Murakami (1984) analyzed the deep convective clouds over the western Pacific and southeast Asia during northern hemisphere summer on intraseasonal time scale. He showed existence of major intraseasonal variation with the 30-40 day periodicity. Lorenc (1984) through EOF analysis of the 200 mb velocity potential field during FGGE year, noticed an eastward propagating divergence wave with zonal wave number 1 on 30-50 day time scale. His results also show the planetary scale eastward propagating mode and smaller scale divergence bands apparently propagating northward over the monsoon region. Singh and Kripalani (1986) through extended EOF analysis noted northward propagation of circulation anomalies on 40-day cycle. Sikka and Gadgil (1980) noted northward movement of the zonally oriented cloud bands from the equatorial Indian Ocean to north India on 30-day time scale.

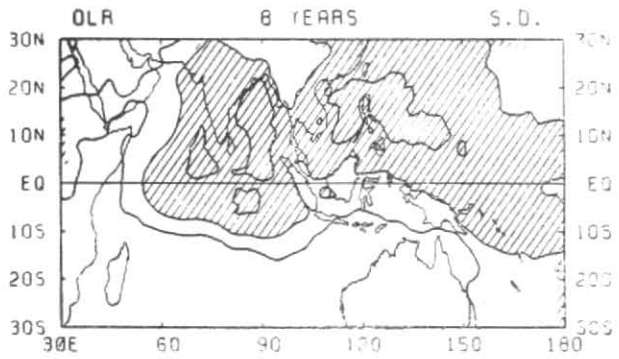

Fig. 1. Standard deviation of OLR′ for eight summers (1 May to 30 Sep 1975-1983, except 1978). Interval is 10 Wm^{-2} with values greater than 30 Wm^{-2} shaded.

Yasunari (1979, 1980) through the spectral analysis of satellite mosaic pictures during the northern hemisphere summer noticed two dominant periodicities around 40-day and 15-day. The fluctuations of 40-day period show marked northward movement of cloudiness from the equatorial zone to the mid-latitudes (around 30°N) over the whole Asiatic monsoon area, and southward movement over Africa and central Pacific. Knutson *et al.* (1986) studied global-scale intraseasonal oscillations during northern hemisphere summer using outgoing longwave radiation and NMC analysis of 250 mb zonal wind. They concluded that 30-60 day mode is the dominant intraseasonal mode of oscillation. Murakami's (1976) analysis of Indian summer monsoon revealed oscillations around 5 days and 15 days. He attributed the 5-day oscillation to monsoon lows and 15-day oscillation to active/break phases of the monsoon.

Recently Lau and Chan (1988) studied the intraseasonal and interannual variations of the tropical convection using OLR. They concluded that the intraseasonal variation in tropical convection is dominated by year round 40-day oscillation which propagate eastward along the equator from the Indian Ocean to the central Pacific. Averaged over the tropics, the 40-day mode variance is about 15% of the total anomaly variance.

Above mentioned observational studies over northern hemisphere summer noted oscillations on three time scales, *i.e.*, 30-60 day, 10-20 day and less than 10-day. Many observational and theoretical studies have focussed on 30-60 day oscillation alone, as it being the strongest mode of intraseasonal variation [Murakami *et al.* (1983), Goswami and Shukla (1984), Chang (1977), Wang (1988) etc]. Most of the previous studies for northern hemisphere summer are based on either small domain or shorter time period. The purpose of this paper is to investigate the temporal and spatial variation of OLR over the Asiatic summer monsoon based on relatively longer period data through EOF analysis.

Empirical orthogonal functions or principal components have so far been used extensively as an aid in climatological investigations. They are of value, however, for two main reasons in that the variance of a scalar field can be represented by comparatively few independent coefficients and the associated patterns may, in some cases, be given a physical interpretation. Principal components are the most efficient set of orthogonal functions in that they represent a given fraction of the variance of a meteorological field with the least number of coefficients. They are derived as the eigenvectors of the covariance matrix between the variables, so that their form depends directly on the coherence of the departures from normal over the area of analysis. The contribution of any component to the total variance of the field is given by the corresponding eigenvalue and provides a convenient measure of its relative importance. In most cases the similar time variation at neighbouring points allows the major part of the variance of the field to be represented by a relatively small number of orthogonal components, with the remainder expressing smaller-scale variations and noise. This comparatively small set of components then expresses the most important mode of variation of the field with time and provides a convenient basis for statistical forecasting and climatological studies (Kidson 1975). Data and computational procedure are discussed in section 2. Section 3 is devoted to discussion of results. Final conclusions are made in section 4.

2. Data and computational procedure

In this study I use daily OLR, measured by scanning radiometers aboard NOAA polar orbiting satellites, covering summers (1 May to 30 September) of 1975 to 1983, except 1978. OLR has been widely used as a representative of convective activity. In the tropics, where surface temperature contrasts are relatively small in most areas, low OLR values correspond to regions of high cloudiness associated with deep convection.

Introducing over bar ($\bar{}$) to represent five month mean and an asterisk ( )* to represent departure from it, the variable OLR can be expressed as :

$$\mathrm{OLR} = \overline{\mathrm{OLR}} + \mathrm{OLR}^* \qquad (1)$$

Thus OLR* represents the transient component of OLR. OLR* can be separated into two components as follows :

$$\mathrm{OLR}^* = a + b\ (t - t_0) + c\,(t - t_0)^2 + \mathrm{OLR}' \qquad (2)$$

where t_0 correspond to 16th of July (middle of the 5-month period). The sum of the first three terms represents the seasonal trend of OLR*, the coefficients a, b and c are determined from a least square method. Accordingly, OLR′ is associated with intraseasonal transient variations. OLR′ values are used for all computations in this paper. Standard deviations of OLR′ reflect the activity of OLR transient disturbances on intraseasonal time scale. The spatio-temporal variation of these OLR′ fields are studied through EOF analysis. In order to be able to perform EOF analysis on the computer facilities available at University of Hawaii, the grid resolution of OLR′ was reduced to 10° Long. × 5° Lat. staggered grid. Then OLR′ values are normalized before subjecting to EOF analysis.

A brief outline of EOF analysis is given here. For details the reader is referred to Grimmer (1963) and Kutzbach (1967). Let f_n be an M component vector representing the n^{th} observation of M variables. Then f_n may be expressed as :

$$f_n = \sum_{i=1}^{M} C_{in}\, e_i \ : n = 1, 2, \ldots\ldots, N \qquad (3)$$

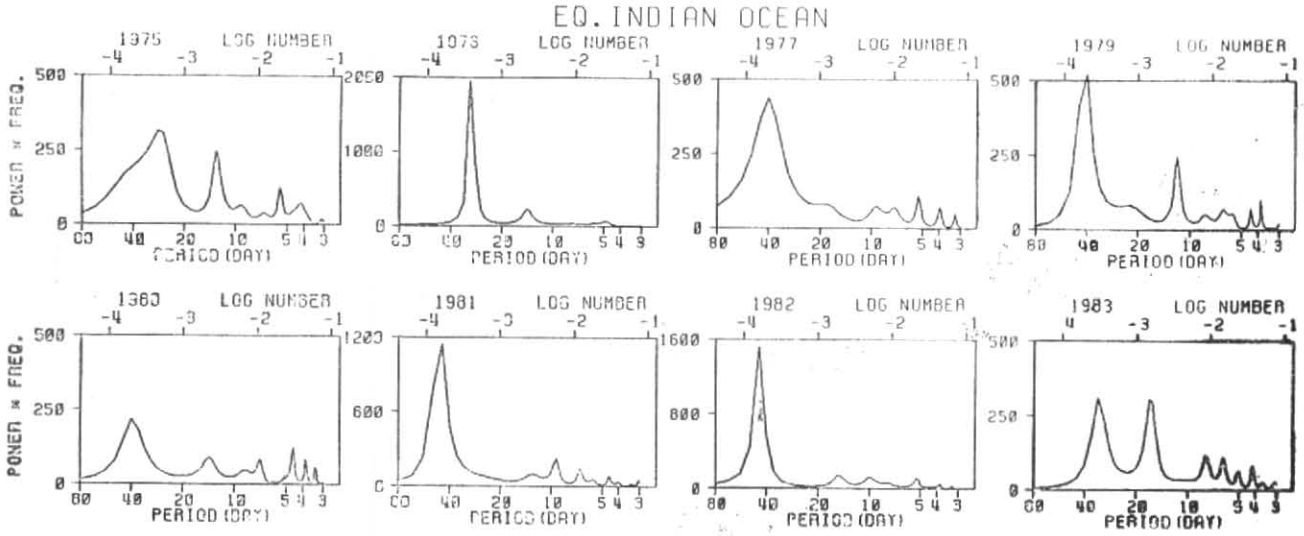

Fig. 2(a). Power spectra of OLR′ for eight summers (1 May to 30 Sep 1975-1983, except 1978) for the Eq. Indian Ocean

where e_i denotes an eigenvector associated with the i^{th} eigenvalue, and C_{in} is the coefficient of the i^{th} eigenvector for the n^{th} observation. The eigenvectors and their associated eigenvalues represent solutions of a maximization of the explained variance problem. The fraction of the total variance explained by the k largest eigenvalues V_k can be obtained from :

$$V_k = \sum_{i=1}^{k} \lambda_i \Big/ \sum_{i=1}^{M} \lambda_i \qquad (4)$$

where, λ_i represents the i^{th} eigenvalue. Here the total number of observations N is equal to 1224, and the total number of variables $M = 202$.

For spectral analysis, the Maximum Entropy Method (MEM) is applied to daily data (OLR′ in the case of regional spectral analysis and C_1 to C_4 in the case of EOF analysis) of each summer (1 May to 30 September) of 1975 to 1983, except 1978. This method has an advantage of giving high resolution, especially for short time record (*e.g.*, Ulrych and Bishop 1975). In the present analysis, the length of the prediction error coefficient of 30 days is used.

3. Results and discussion

Fig. 1 shows the standard deviation of the seasonal mean and seasonal trend removed daily outgoing longwave radiation (OLR′). It clearly shows high standard deviation values over the equatorial Indian Ocean, Bay of Bengal and northwest Pacific, which indicates that intraseasonal activity is strong over these regions. Sikka and Gadgil (1980) noticed that maximum cloud zone from the equatorial Indian Ocean move northward and occupy the monsoon trough position on intraseasonal time scale. The path of the northward movement of these maximum cloud zones coincide with location of high standard deviation values in Fig. 1. This indicates that fluctuations in the activity of Indian monsoon occur due to northward movement of cloud clusters from the equatorial Indian Ocean. Another region of high standard deviation values of OLR occur in the northwest Pacific and south China Sea. This may correspond to the northward and southward movement of the monsoon trough over this region during northern hemisphere summer. The high values of standard deviation over the northwest Pacific may be due to frequent passage of synoptic scale disturbances over that region. Murakami (1984) noticed spectral peaks on the time scales of 3 to 4, 7 to 9 and 30 to 40 days in the activity of cloudiness over this region.

Of particular interest is high standard deviation values over the northwest Pacific, Philippine Sea and south China Sea region with a discontinuity over the Philippine islands. The region of high standard deviation values over south China Sea coincides with the region where both southward propagating disturbances from the Tibetan plateau and northward propagating disturbances from the Indonesian islands meet on 30-60 day time scale (Murakami 1984). By and large, the region of high standard deviation values (Fig. 1) coincide with the regions where 30-60 day and 10-20 day oscillations are strong. Two regions of high standard deviation, one in the equatorial Indian Ocean (5° S-10° N, 65° -95° E) and the other in the northwest Pacific (10° -25° N, 110° -140° E), are selected and are subjected to spectral analysis. Though the standard deviation is not high over the Indian region, a small region covering Peninsular India and Bay of Bengal (10°-22.5° N, 70°-95° E) is selected out of authors special interest to Indian region and subjected to spectral analysis.

The spectral analysis of the Indian Ocean region is shown in Fig. 2(a). This figure shows spectral peaks around 45 days almost every year and spectral peaks between 10 & 20 days during 1975, 1979 and 1983 summers. The years of strong 45-day spectral peak (1976, 1977, 1981 and 1982) do not show any spectral peak around 15 days whereas years of weak 45-day spectral peak show second spectral peak around 15 days. Madden and Julian (1971) using zonal wind and surface pressure at Canton Island noticed spectral peaks around 40-50 day period. They suggested that this oscillation is a result of eastward propagating circulation cell oriented in the equatorial zonal plane (Madden

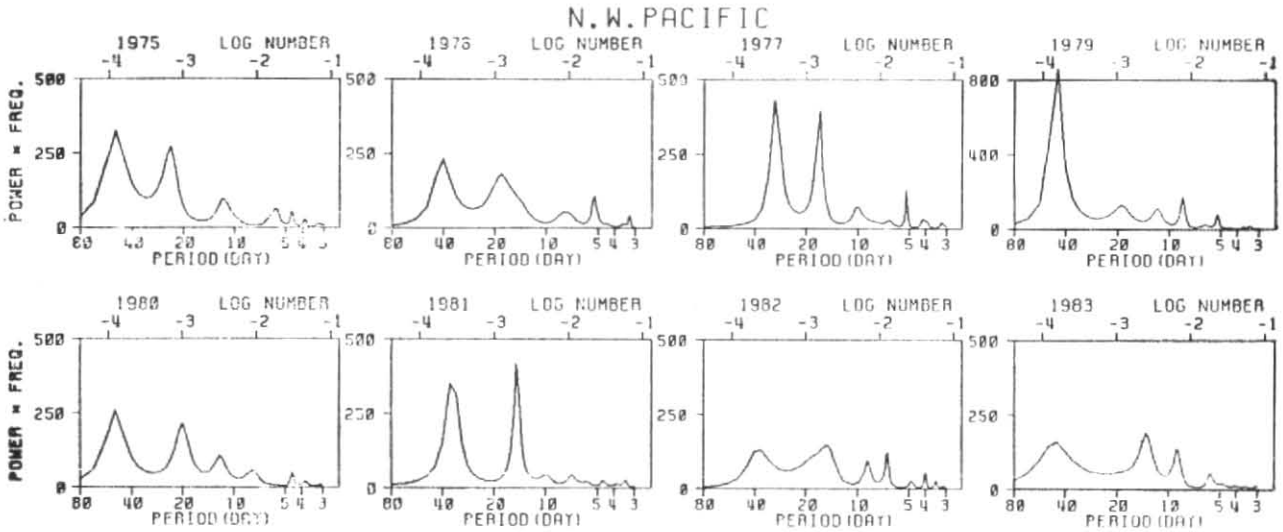

Fig. 2(b). As in Fig. 2(a), except for the northwest Pacific

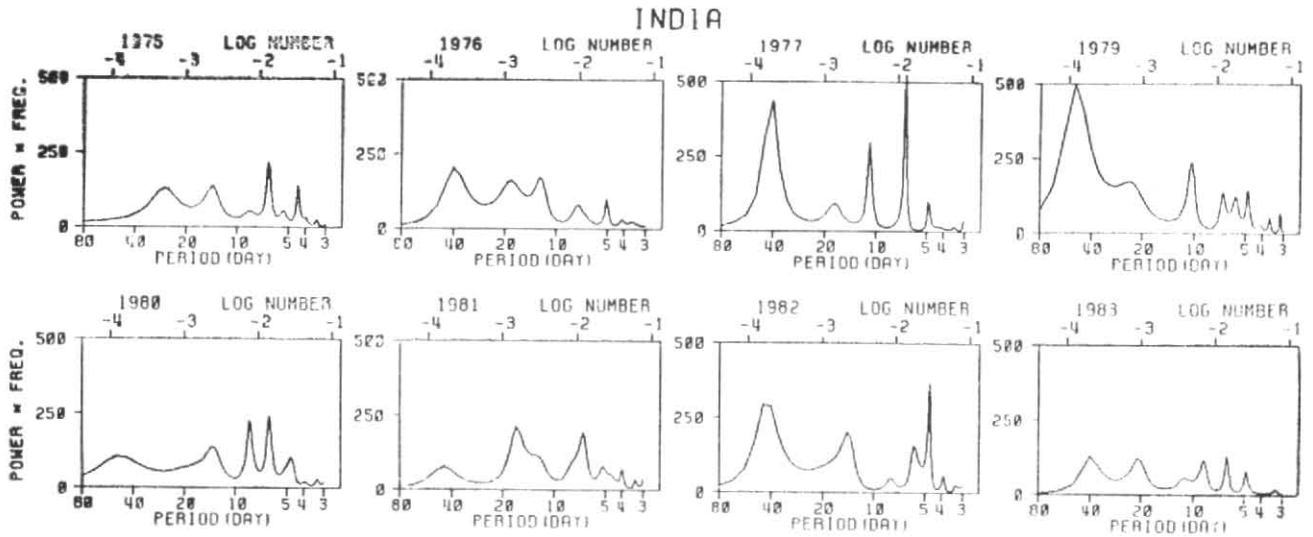

Fig. 2(c). As in Fig. 2(a), except for the Indian region

and Julian 1972). The 45-day spectral peak observed is a part of the global-scale eastward propagating circulation cell noticed by Madden and Julian (1972). After Madden and Julian (1971, 1972), the so called 40-50 day (later on extended to 30-60 day) oscillation has been widely studied. Of particular interest during 1976 and 1982 is very large power (compare the scales of y-axis) explained by the 45-day mode and almost negligible power explained by the 15-day mode. This clearly indicates that 45-day mode is the dominant mode in the equatorial Indian Ocean. Lau and Chan (1985) suggested that the 40-50 day activity in the equatorial Indian Ocean may have acted as a trigger to the 1982-83 *El Nino* / Southern Oscillation (ENSO) event. Two ENSO events, one in 1976-77 and the other in 1982-83, occurred during this study period. In this study, sharp spectral peaks around 40 days in the equatorial Indian Ocean during the preceding summer of ENSO (1976 and 1982) provide some kind of evidence for Lau and Chan's (1985) suggestion.

Fig. 2 (b) shows the spectrum analysis of the northwest Pacific. This figure shows at least two spectral peaks centred around 45 and 15 days every year except 1979. Unlike the equatorial Indian Ocean (Fig. 2a) the power explained by the 45-day mode is very small during 1976 and 1982 summers. On the other hand, the power explained by the 15-day mode is large in the northwest Pacific than in the equatorial Indian Ocean. This suggests that for the onset phase of ENSO, short period fluctuations from the northwest Pacific and 45-day fluctuations from the equatorial Indian Ocean are important. Further research is needed to support this idea.

Fig. 2(c) shows the power spectrum analysis of OLR′ over Indian region. The discussion of this figure is made with regard to activity of the Indian summer monsoon rainfall averaged over the subdivisions fall approximately under this region. Here the Indian summer monsoon rainfall is divided into three categories, *viz.*, near normal, above normal and below normal. In this study period, 1976, 1977 and 1981 fall under near normal rainfall category, 1975, 1980 and 1983 fall under above normal rainfall category and 1979 and 1982 fall under below normal rainfall category.

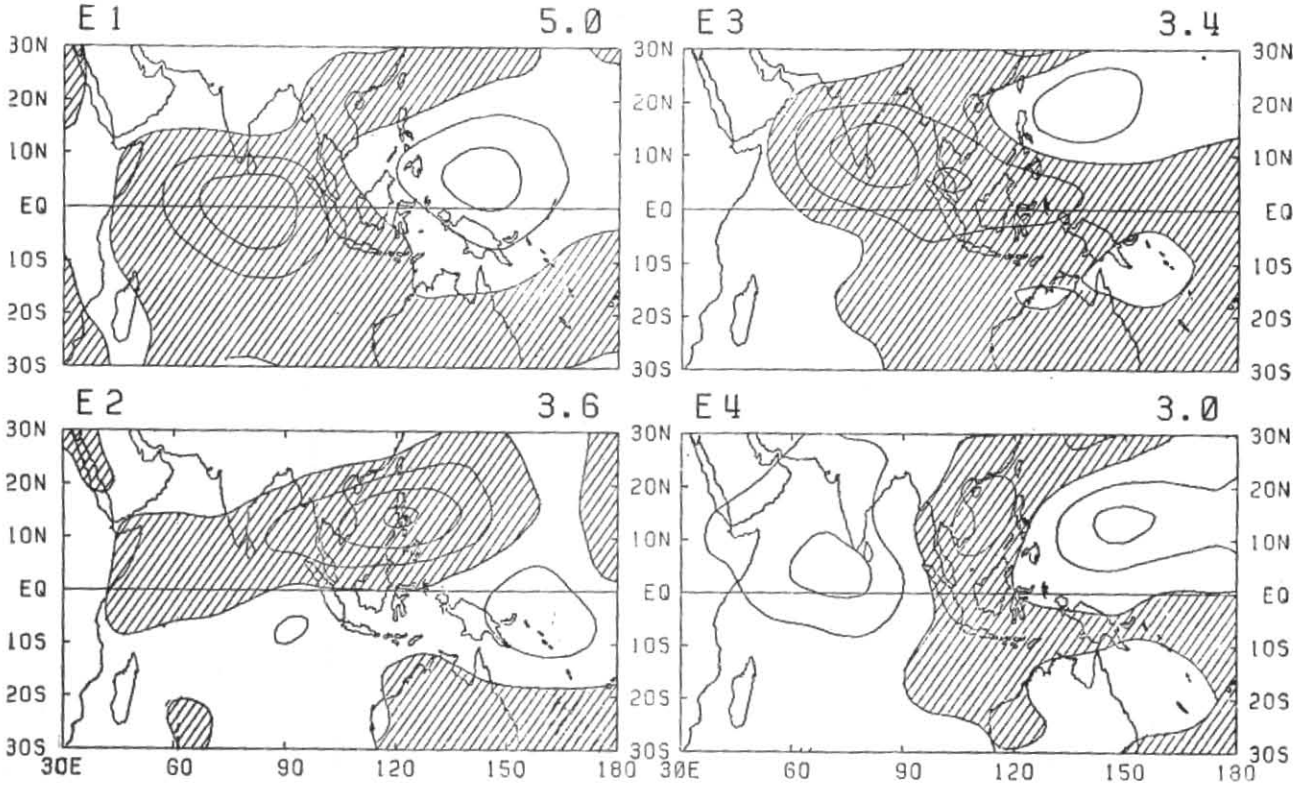

Fig. 3. First four (E_1 to E_4) eigenvector fields (multiplied by 100) obtained from daily OLR′ for eight summers (1 May to 30 Sep 1975-1983, except 1978). The percentage of variance explained by each mode is shown at the top of the diagram. Interval is 5 units with positive values shaded

During the near normal monsoon years (1976, 1977 and 1981), spectral peaks on time scales 45, 15 and 7 days are apparent. 45-day and 15-day cycles may be associated with the active and break phases of the Indian monsoon activity. Krishnamurti and Bhalme (1976) noticed quasi-biweekly cycle and 2-6 days fluctuations in near normal active monsoon system. They attributed this quasi-biweekly cycle to the active and break phases of the monsoon system. Murakami (1976) observed two major periodicities, *viz.*, 15-day and 5-day in the monsoon activity. He attributed the 15-day cycle to the active and break phases of the Indian summer monsoon, and 5-day cycle to the monsoon lows or monsoon depressions. During above normal monsoon activity years (1975, 1980 and 1983), there is not much power in the 45-day or 15-day cycle, instead there is some power in the high frequency side, *i.e.*, less than 10 days. This indicates that during very active monsoon years, there are no breaks in the monsoon activity and most of the rainfall comes from the disturbances less than 10 days, *i.e.*, monsoon depressions. Monsoon depressions, the main rain producing disturbances during the Indian summer monsoon, are responsible for almost 70% of the Indian summer monsoon rainfall. During below normal monsoon years (1979 and 1982). spectral peaks on time scales of 45 and 15 days are apparent. This suggests that bad monsoon activity or drought years are associated with long lasting breaks in the monsoon activity over the Indian region.

Fig. 2(c) suggests that, by and large, breaks in the monsoon activity occur on two time scales, *i.e.*, either centred around 45 days or 15 days. Some times 45-day signal may not be strong (ex. 1981). The short period breaks (15-day) are associated with normal monsoon activity and long period breaks (45-day) are associated with bad monsoon activity over Indian region. There are no breaks in the monsoon activity during flood years. It is important to bear in mind that the long lasting breaks may not be continuously dry for the entire period of 15-30 days within the 30-60 day cycle. During this period there may be less intense active spells occasionally. Though there is a strong 45-day signal during 1977 summer, short period fluctuations make 1977 summer near normal active instead of below normal active. This suggests that phase locking of waves on different time scales is responsible for the activity of a monsoon system. Krishnamurti *et al.* (1985) suggested that the 30-50 day eastward propagating planetary-scale divergence and sea level pressure waves, the 10-20 day westward propagating pressure perturbation and meridionally propagating 30-50 day trough lines, associated divergences, all modulate the monsoon. Of particular interest in Figs. 2 (b) and 2 (c) is as we go away from the equator towards higher latitude, the power in the low frequency (30-60) side decreases. This indicates that the so called 30-60 day oscillation is confined more to equatorial latitudes than higher latitudes.

In the above discussion, I have shown spectral analysis for three small regions only. These three regions show the existence of oscillations on at least three time scales. However, Asiatic summer monsoon is a large-scale phenomenon. In order to see whether the source of these oscillations is of local or global, EOF analysis is performed.

The first four EOF components of the OLR anomalies are presented in Fig. 3. These four eigenvectors account for 5.0, 3.6, 3.4 and 3.0 of the total variance in order

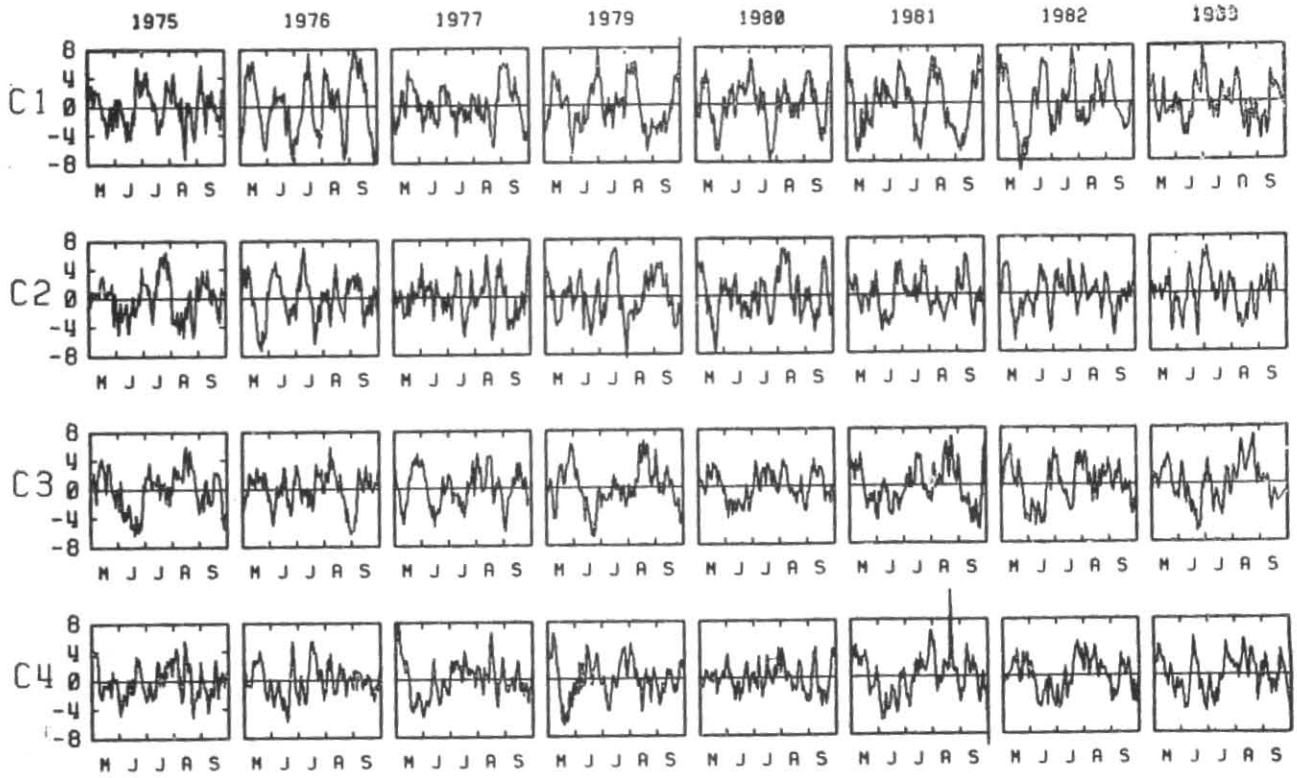

Fig. 4. Time coefficients of the first four eigenvectors (C_1 to C_4)

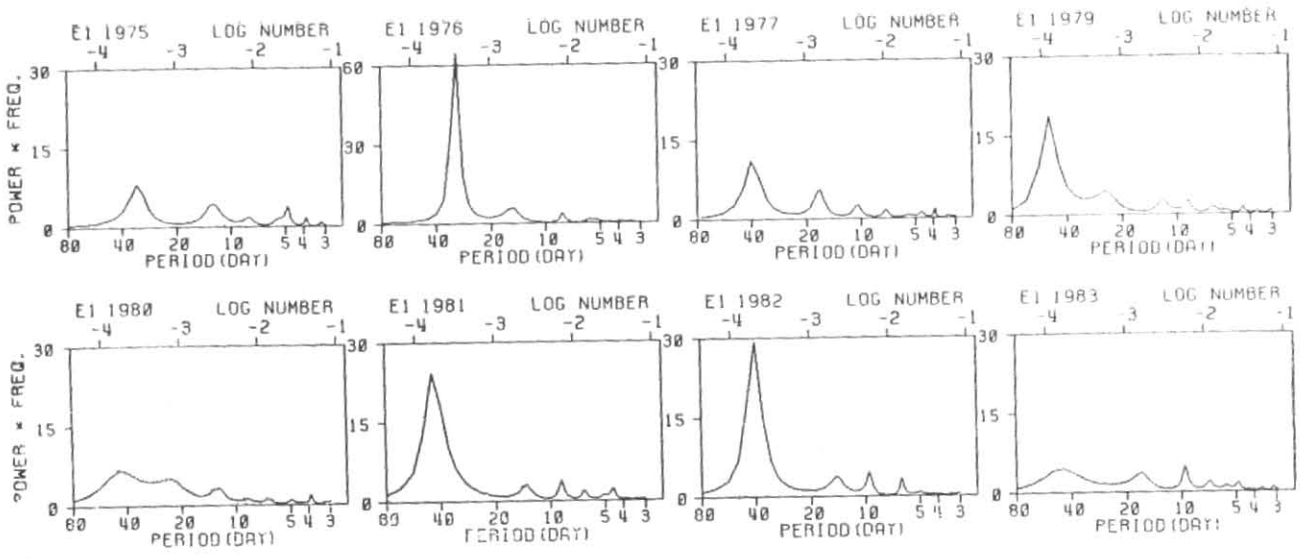

Fig. 5(a). Power spectra of C_1 for eight summers (1 May to 30 Sep 1975-1983, except 1978)

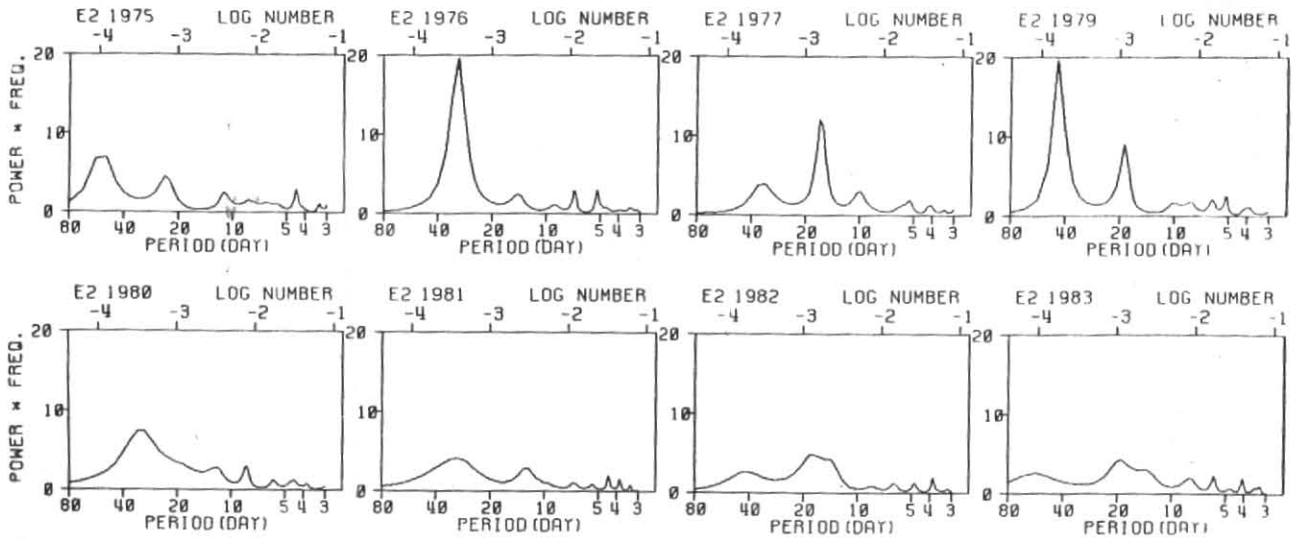

Fig. 5(b). As in Fig. 5(a), except for C_2

The small variance explained by the first four eigenvectors is due to the daily data used in the analysis. The first eigenvector clearly shows two centres of action without of phase relationship. One centre is located over the equatorial Indian Ocean around 90° E and the other is located over the northwest Pacific around 140° E. This feature is similar to the east-west dipole pattern noticed by Lau and Chan (1985). They suggested that this east-west dipole pattern near equator propagates from the Indian Ocean towards the western and central Pacific. This feature indicates that when the equatorial Indian Ocean is at its dry phase, the northwest Pacific is at its wet phase and *vice versa*. The second component has a strong centre of action over S. China Sea-Philippine Sea with an opposite, less intense centre over equatorial western Pacific.

The component three shows major activity along the Asian summer monsoon trough, *i.e.*, the major activity region extends from India, Indochina to maritime continent. This pattern very well agrees with long term mean cloud pattern for the month of June (Atkinson and Sadler 1970). From this pattern and time coefficients, it is clear that the OLR anomalies are always below normal in the month of June. This indicates that this pattern is typical of the onset phase of the Asiatic summer monsoon. The shaded region in this figure agrees very well with the high percentage of variance explained by 30-50 day mode of low level (850 mb) wind field (Krishnamurti and Gadgil 1985, Fig. 4b). The fourth component shows pattern having much smaller scale features. The discussion of this component is omitted because of the small-scale features.

Fig. 4 shows the time coefficients (C_1 to C_4) of the first four eigenvectors. Through eye ball movement one can see periodicity in the range of 30-60 day during 1976, 1979, 1980, 1981 and 1982 of C_1. As we go to higher mode time coefficients, though some kind of periodicity is seen during 1976 and 1979, it is very difficult to make out the time scale. In order to be able to make out the periodicity clearly, spectral analysis is performed for every summer and for each time coefficient separately. The power spectra of each time coefficient are shown in Figs. 5(a)-(d).

It is clear from Fig. 5(a) that the spectral power in the 30-60 day time scale is large and is greater than 15-day cycle. The spectral power in the high frequency side is almost negligible. This means first eigen mode selects large scale features which oscillate on longer time scale. This points out the advantage in performing EOF analysis to notice the oscillations associated with large-scale features.

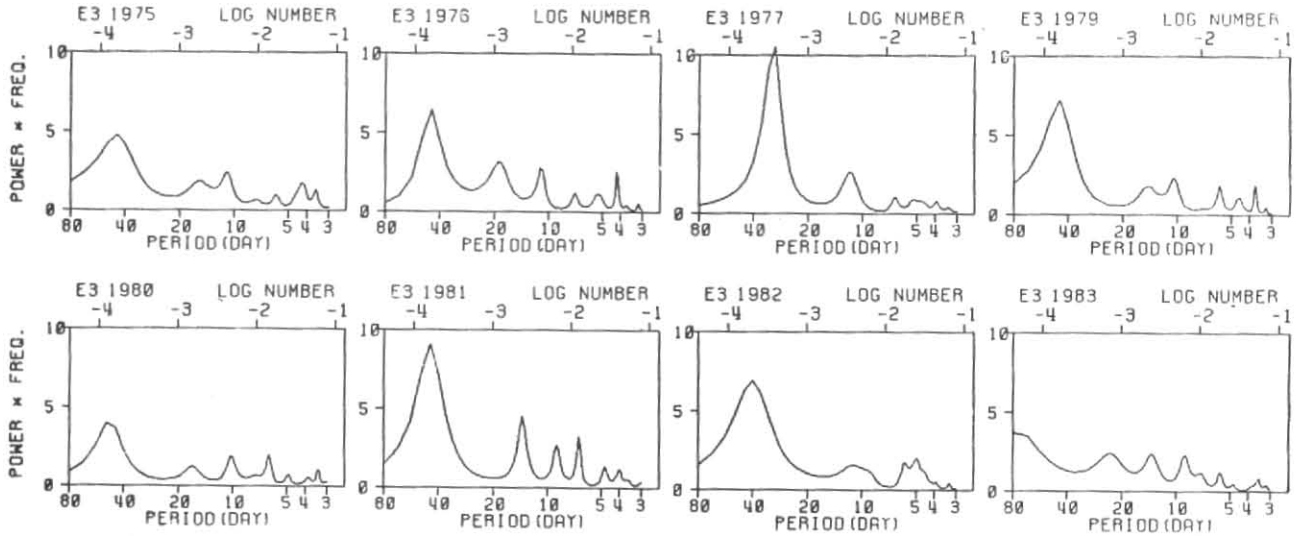

Fig. 5(c). As in Fig. 5(a), except for C_3

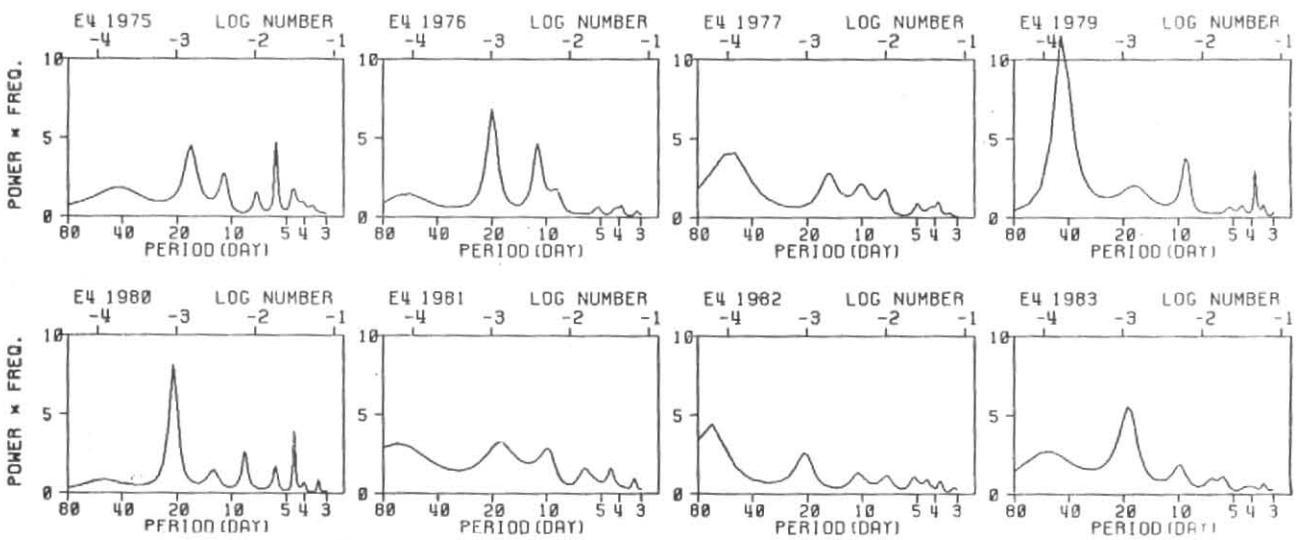

Fig. 5(d). As in Fig. 5(a), except for C_4

Over all from Fig. 5(a) it can be concluded that the first eigen mode shows strong power around 30-60 day during 1976, 1979, 1981 and 1982 and weak power during 1975, 1977 and 1983. 1980 shows weak power over a broad band ranging from 20 to 60 days. Out of 8 years studied, at least 6 years show periodicity around 30-60 days. Since first eigen mode explains the maximum variance, it can be concluded that 30-60 day oscillation is the strongest mode of oscillation on the intraseasonal time scale over the Asiatic summer monsoon. This is in agreement with the previous results.

The spectra of C_2 are shown in Fig. 5(b). The spectrum of 1976 shows a clear 30-day cycle. The spectrum of 1979 shows peaks around 40-day and 20-day, while the spectrum of 1977 shows a peak at 15 days. The spectrum of 1980 shows a broad peak around 30 days. Over all, the second eigen mode shows periodicities on different time scales in different years. Some years show periodicities on two time scales ranging from 15 to 50 days.

The spectra of the time coefficients of C_3 are shown in Fig. 5(c). It is clear from this figure that every year except 1983 show periodicity in the range of 30-60 days, with 1976, 1977, 1979, 1981 and 1982 having sharp spectral peaks. Over all, every year, except 1983 show power in the period range of 30-60 days. This means third eigen mode is dominated by 30-60 day time scale. Recalling the pattern of third eigenvector, it is clear that the maximum activity in this mode is along the Asiatic summer monsoon trough region. From the spectrum of C_3 and E_3 pattern it is clear that the 30-60 day mode occurs almost every summer over the Asiatic summer monsoon. This result is in agreement with Krishnamurti and Gadgil's (1985) result who showed that 30-60 day variance of 850 mb U-component is large along the Asian summer monsoon trough. Satellite infrared radiance data analyzed by Smith and Sikka (1987) also showed that on 30-60 scale the fluctuation of monsoon rainfall over India and radiances are coherent.

From the time coefficient of the fourth eigen mode (Fig. 4) it is clear that shorter time scale fluctuations are dominant in this mode. The power spectra of C_4 is shown in Fig. 5(d). This figure shows spectral peaks around 10 and 20 days every year. Only 1979 shows spectral peak around 40 days. One important thing to be noticed from Figs. 5(a)-5(d) is, as we go to the higher mode, both spatial and temporal scale of the oscillation decreases.

4. Concluding remarks

This study presents the intraseasonal variations of the Asiatic summer monsoon based on relatively longer period of OLR data. The intraseasonal variations occur on 30-60 day, 10-20 day and less than 10-day time scales over the Asiatic summer monsoon. This study also shows the interannual variation in the so called 30-60 day oscillation. The 30-60 day oscillation is strong in the Indian Ocean during the preceding summers of ENSO events. There is a suggestion of possible link between 30-60 day mode and ENSO.

The active and break phases of the Indian monsoon occur on two time scales, *viz.*, 10-20 day and 30-60 day. When the 10-20 day oscillation together with short period oscillation exists, the over all summer monsoon activity is near normal and when the 30-60 day oscillation together with 10-20 day oscillation exists, the over all summer monsoon activity is below normal. Some times the 30-60 day oscillation together with short period disturbances may make the monsoon activity near normal. This study calls for further research on phase locking of different waves on both intraseasonal and interannual time scales. The limitations of this study are (*i*) the variance explained by the first four eigenvectors is only 15% and (*ii*) the Indian summer monsoon activity estimate is very crude and comparison of this estimate with spectral analysis should be taken in a large scale sense.

Acknowledgements

The author is indebted to Prof. Takio Murakami for his guidance throughout the course of this work. This research was supported by the National Science Foundation under grant ATM-86-09968.

References

Atkinson, G.D. and Sadler, J.C., 1970, *Mean cloudiness and gradient level wind charts over the Tropics.* Volume II. U.S. Air Force, Tech. Rep. 215, Vol. II, Charts 48.

Cadet, D., 1983, The monsoon over the Indian Ocean during summer 1975—Part II : Break and active monsoons, *Mon. Weath. Rev.*, **111**, 95-108.

Chang, C.P., 1977, Viscous internal gravity waves and low-frequency oscillations in the tropics, *J. atmos. Sci.*, **34**, 901-910.

Grimmer, M., 1963, The space-filtering of monthly surface temperature anomaly data in terms of pattern, using Empirical Orthogonal Functions, *Quart. J. R. met. Soc.*, **89**, 395-408.

Goswami, B.N. and Shukla, J., 1984, Quasi-periodic oscillations in a symmetric general circulation model, *J. atmos. Sci.*, **41**, 20-37.

Kidson, J. W., 1975, Eigenvector analysis of monthly mean surface data, *Mon. Weath. Rev.*, **103**, 177-186.

Knutson, T. R., Weickmann, K. M. and Kutzbach, J. E., 1986, Global-Scale intraseasonal oscillations of Outgoing Longwave Radiation and 250 mb zonal wind during Northern Hemisphere summer, *Mon. Weath. Rev.*, **114**, 605-623.

Krishnamurti, T.N. and Bhalme, H.N., 1976, Oscillations of a monsoon system-Part I : Observational aspects, *J. atmos. Sci.*, **33**, 1937-1954.

Krishnamurti, T.N. and Gadgil, S., 1985, On the structure and maintenance of the 30 to 50 day mode over the globe during FGGE, *Tellus*, **37A**, 336-360.

Krishnamurti, T.N., Jayakumar, P.K., Sheng, J., Surgi, N. and Kumar, A., 1985, Divergent circulations on the 30 to 50 day time scale, *J. atmos. Sci.*, **42**, 364-375.

Kutzbach, J.E., 1967, Empirical Eigenvectors of sea-level pressure, surface temperature and precipitation complexes over North America, *J. appl. Met.*, **6**, 791-802.

Lau, K.M. and Chan, P.H., 1988, Intraseasonal and interannual variations of tropical convection : A possible link between the 40-50 day mode and ENSO, *J. atmos. Sci.*, **45**, 506-521.

Lau, K.M. and Chan, P.H., 1985, Aspects of the 40-50 day oscillation during the northern winter as inferred from outgoing longwave radiation, *Mon. Weath. Rev.*, **113**, 1889-1909.

Lorenc, A.C., 1984, The evolution of planetary scale 200 mb divergences during the FGGE year, *Quart. J. R. met. Soc.*, **110**, 427-441.

Madden, R.A. and Julian, P.R., 1971, Detection of a 40-50 day oscillation in the zonal wind in the tropical Pacific, *J. atmos. Sci.*, **28**, 702-708.

Madden, R.A. and Julian, P.R., 1972, Description of global-scale circulation cells in the tropics with a 40-50 day period, *J. atmos. Sci.*, **29**, 1109-1123.

Murakami, M., 1984, Analysis of the deep convective activity over the western Pacific and Southeast Asia—Part II : Seasonal and intraseasonal variations during northern summer, *J. met. Soc. Japan*, **62**, 88-108.

Murakami, M., 1976, Analysis of summer monsoon fluctuations over India, *J. met. Soc. Japan*, **54**, 15-31.

Murakami, T., 1980, Empirical Orthogonal Function analysis of satellite observed Outgoing Longwave Radiation during summer, *Mon. Weath. Rev.*, **108**, 205-222.

Murakami, T., Nakazawa, T. and He, J., 1983, On 40-50 day oscillations during Northern Hemisphere summer, Tech. Rep. No. UHMET 83-02, Dep. of Met., Univ. of Hawaii.

Sikka, D.R. and Gadgil, S., 1980, On the maximum cloud zone and the ITCZ over Indian longitudes during the South West monsoon, *Mon. Weath. Rev.*, **108**, 1840-1853.

Singh, S.V. and Kripalani, R.H., 1986, Application of Extended Empirical Orthogonal Function analysis to interrelationships and sequential evolution of monsoon fields, *Mon. Weath. Rev.*, **114**, 1603-1610.

Smith, E.A. and Sikka, D.R., 1987, Coherence of satellite infrared temperatures with monsoon rainfall at preferred frequencies and triplex behaviour of the Indian summer monsoon, *Met. atmos. Phys.*, **37**, 219-236.

Ulrych, T.J. and Bishop, T.N., 1975, Maximum entropy spectral analysis and autoregressive decomposition, *Rev. Geophys. and Space Phys.*, **13**, 183-200.

Wang, B., 1988, Dynamics of tropical low-frequency waves : An analysis of the moist Kelvin wave, *J. atmos. Sci.*, **44**, 2052-2065.

Yasunari, T., 1979, Cloudiness fluctuations associated with the northern hemisphere summer monsoon, *J. met. Soc. Japan*, **57**, 227-242.

Yasunari, T., 1980, A quasi-stationary appearance of 30-40 day period in the cloudiness during the summer monsoon over India, *J. met. Soc. Japan*, **58**, 225-229.